Available online at www.sciencedirect.com
ScienceDirect
Geochimica et Cosmochimica Acta 71 (2007) 974–983
Geochimica
www.elsevier.com/locate/gca

Activity–composition relations in the system $CaCO_3$–$MgCO_3$ predicted from static structure energy calculations and Monte Carlo simulations

Victor L. Vinograd [a,*], Benjamin P. Burton [b], Julian D. Gale [c], Neil L. Allan [d], Björn Winkler [a]

[a] *Institut für Geowissenschaften, Universität Frankfurt, Frankfurt a.M., Germany*
[b] *Ceramics Division, National Institute of Standards, Gaithersburg, USA*
[c] *Nanochemistry Research Institute, Curtin University of Technology, Perth, WA, Australia*
[d] *School of Chemistry, University of Bristol, Bristol, UK*

Received 12 July 2006; accepted in revised form 1 November 2006

Abstract

Thermodynamic mixing properties and subsolidus phase relations of the rhombohedral carbonate system, $(1-x)\cdot CaCO_3 - x\cdot MgCO_3$, were modelled in the temperature range of 623–2023 K with static structure energy calculations based on well-parameterised empirical interatomic potentials. Relaxed static structure energies of a large set of randomly varied structures in a $4\times4\times1$ supercell of $R\bar{3}c$ calcite ($a = 19.952$ Å, $c = 17.061$ Å) were calculated with the General Utility Lattice Program (GULP). These energies were cluster expanded in a basis set of 12 pair-wise effective interactions. Temperature-dependent enthalpies of mixing were calculated by the Monte Carlo method. Free energies of mixing were obtained by thermodynamic integration of the Monte Carlo results. The calculated phase diagram is in good agreement with experimental phase boundaries.

1. Introduction

The rhombohedral calcite–magnesite binary, $(1-x)\cdot CaCO_{1-x}\cdot MgCO_3$, is one of the most well studied solid solutions in mineralogy. The experimental study of Goldsmith and Heard (1961) identified the essential features of subsolidus phase relations: two asymmetric miscibility gaps separated by a narrow stability field for the dolomite-structure phase. Calorimetric studies by Navrotsky and Capobianco (1987), Chai et al. (1995), Chai and Navrotsky (1996), and Navrotsky et al. (1999) showed that the enthalpy of formation of ordered dolomite is negative, relative to a mechanical mixture of calcite and magnesite, but the formation enthalpy for a disordered solid solution of the same composition is positive; consistent with theoretical studies of Burton and Kikuchi (1984) and Burton (1987). The magnitude of the enthalpy of disorder is uncertain owing to different calorimetric results: 1.23 ± 0.32 kJ/mol (Navrotsky and Capobianco, 1987) for a heat-treated natural sample; and 16.5 ± 2.5 kJ/mol (Navrotsky et al., 1999) for a synthetic sample. Burton and Van de Walle (2003) published an extensive data set of formation energies for various ordered supercells, that were calculated with the Vienna ab initio simulation package, VASP (Kresse and Hafner, 1993; Kresse, 1994; Kresse and Furthmüller, 1996). The VASP calculations also yield a negative formation energy for dolomite and first principles phase diagram calculations based on the VASP formation energies yield an enthalpy of mixing of ~6 kJ/mol for the random solid solution at $x = 0.5$. Various theoretical approaches including the Bragg–Williams model (Navrotsky, 1987; Davidson, 1994), different approximations of the cluster variation method (Burton and Kikuchi, 1984; Burton, 1987) and

* Corresponding author. Fax: +49 69 798 22101.
E-mail address: v.vinograd@kristall.uni-frankfurt.de (V.L. Vinograd).

0016-7037/$ - see front matter © 2006 Elsevier Inc. All rights reserved.
doi:10.1016/j.gca.2006.11.008

Monte Carlo simulations (Burton and Van de Walle, 2003; Purton et al., 2006) achieve qualitative or semi-quantitative agreement between predicted and experimentally determined phase relations. However, none of these studies produced a mathematically simple activity–composition model consistent with experimental phase boundaries. Such a model is often requested for petrological and environmental studies which attempt phase equilibrium calculations in chemically complex systems. Here we derive activity–composition relations for the temperature range of 623–1323 K with static structure energy (SSE) calculations based on the well parameterised set of empirical interatomic potentials of Rohl et al. (2003) and Austen et al. (2005). Calculations were performed in the following sequence:

- Testing the empirical interatomic potentials.
- SSE calculations on a large set of randomly varied structures.
- Fitting a cluster expansion, CE, to the SSE, i.e. finding a mathematically simple equation that fits the excess SSE.
- Ground state analysis, i.e. finding the structures with lowest SSE.
- Monte Carlo simulations of temperature-dependent properties.
- Thermodynamic integration of the Monte Carlo results to calculate free energies of mixing.
- Fit a polynomial to the Monte Carlo free energies and calculate activity–composition relations.

This sequence of calculations yields activity–composition relations that agree almost quantitatively with the experimentally determined phase relations.

2. Empirical potentials

Rohl et al. (2003) and Austen et al. (2005) developed a set of interatomic potentials for carbonate minerals, which exhibit remarkable accuracy in reproducing the structures of calcite, dolomite, magnesite, and aragonite as well as available elastic stiffness data on calcite and magnesite. However, a good description of the structure and elasticity data does not guarantee accurate predictions of energy differences between differently ordered supercells. To test the force-field-based SSEs, we compare them to DFT–SSE for the same set of ordered structures, that Burton and Van de Walle (2003) considered. In Fig. 1 we plot the FF–SSE vs. VASP–SSE. The FF–SSE calculations were done using the program GULP (Gale, 1997; Gale and Rohl, 2003). The plot includes all structures described by Burton and Van de Walle (2003) except for the huntite, $Ca_3Mg(CO_3)_4$ structure, for which FF–SSE = 28.72 kJ/mol and DFT–SSE = 44.73 kJ/mol. This large difference in excess energy is related to the difference between CO_3-group orientations in huntite vs. that in calcite and magnesite. The good correlation between the FF- and DFT–SSE sets suggests that the Austen et al. (2005) potentials essentially reproduce the energetics of cation mixing/ordering.

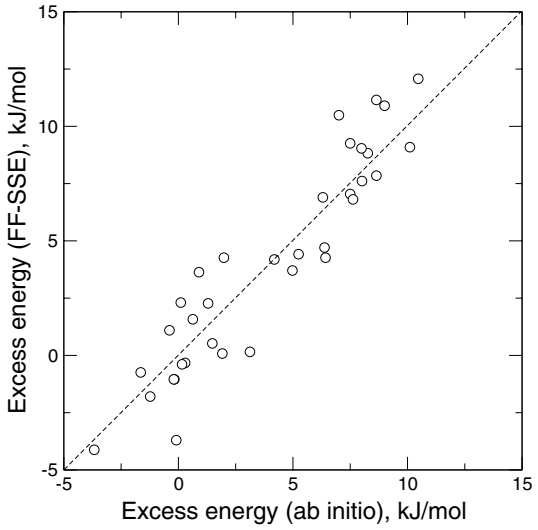

Fig. 1. Correlation between the excess energies of a selected set of ordered structures calculated with parameterized force field (Austen et al., 2005) and VASP (Burton and Van de Walle, 2003) methods. The dashed line corresponds to an ideal correlation.

3. Supercell SSE calculations

We use a $4 \times 4 \times 1$ supercell of $R\bar{3}c$ calcite ($a = 19.952$ Å, $c = 17.061$ Å) that contains 96 exchangeable (Ca, Mg) atoms. We start in the ordered dolomite structure, in which Ca and Mg occupy alternate layers perpendicular to the c axis, and generate several structures, with compositions between calcite and magnesite, by replacing appropriate numbers of Ca or Mg atoms with Mg and Ca atoms, respectively. Cation distributions in structures with compositions $x = 0.125$, 0.25, 0.375, 0.5, 0.625, 0.75, and 0.875 were varied by randomly swapping selected atoms pairs. Swapping was repeated 100 times at each composition and fully relaxed static FF–SSEs were calculated for each structure. Excess energies of these 700 structures are plotted in Fig. 2. The excess property is defined relative to the weighted sum of the energies of pure calcite and magnesite. This plot outlines only the general shape and magnitude of the enthalpy of mixing. Calculating enthalpy isotherms requires additional effort.

4. The cluster expansion

Constructing isotherms requires Boltzmann averaging over many configurations at each composition in a sufficiently large supercell. Accurate estimates of the average energies can be made with a Monte Carlo algorithm, but computational efficiency requires more rapid SSE calculations than a fully atomistic force field permits. Therefore, the cluster expansion (CE) method (Connolly and Williams, 1983; Sanchez et al., 1984) is used to speed up calculations. The CE is compact set of effective interactions, which in its simplest form (Dove, 1999; Becker et al., 2000; Vinograd, 2001) maps the excess energy, E_i,

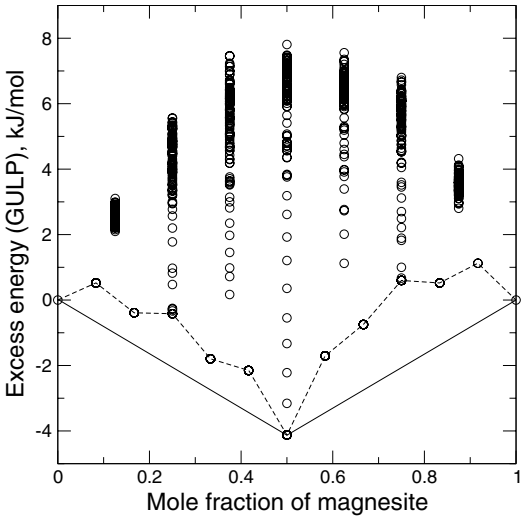

Fig. 2. Excess static structure energies for 700 structures that were calculated with the interatomic potentials of Austen et al., 2005. The dashed line connects minimum energy structures at each composition; calcite, dolomite, and magnesite are the only predicted ground states (solid line).

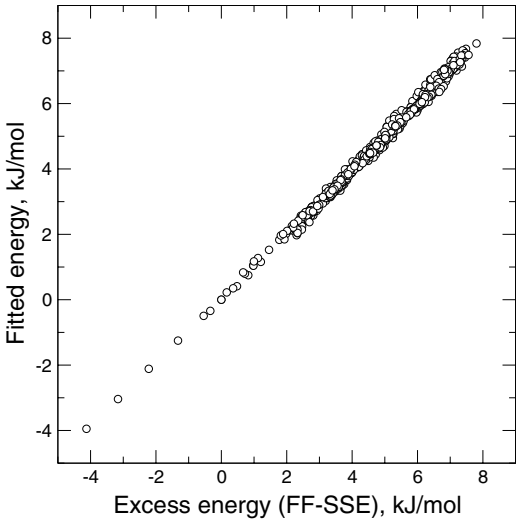

Fig. 3. Correlations between the energies of 700 structures calculated with GULP and those calculated with the cluster expansion. The average absolute deviation of the fitted energies from the FF–SS energies is 3.56 percent.

of structure, i, onto a set of effective pair interactions, $J^{(n)}$, that are coupled to the frequencies of AB pairs, $f_{AB}^{(n)}$ in structure i;

$$E_i = 1/2 \sum_n f_{AB}^{(n)} J^{(n)} + E_0, \quad (1)$$

where n is the order of the near-neighbor pair, which increases with interneighbor separation, and E_0 is a configuration independent strain energy. In solid solutions with size mismatch E_0 represents the global strain that is caused by substituting smaller ions (Mg) into larger-ion-rich (Ca-rich) crystals, or larger ions (Ca) in smaller-ion-rich (Mg-rich) crystals. Ferreira et al. (1988) demonstrated that this strain energy is maximized at an intermediate composition, typically not $x = 0.5$, such that it varies superquadradically with composition. We approximate this variation with a two-parameter polynomial:

$$E_0 = x_1 x_2 (x_1 A_{12} + x_2 A_{21}). \quad (2)$$

For each of the 700 structures we calculated frequencies of AB-type (Mg–Ca) pairs at 12 distances ranging from 3.8 to 10.4 Å. The frequencies and the energies form an overdetermined system of 700 equations, which were solved for $J^{(n)}$, A_{12}, and A_{21} using a least-squares minimization.

Fig. 3 is a plot of excess energies for the 700 structures that were calculated with the CE vs. those calculated with GULP. Each $J^{(n)}$ corresponds to the energy of the exchange reaction Ca–Ca + Mg–Mg = 2Ca–Mg at the nth neighbor distance. Negative Js indicate an ordering tendency (Ca–Mg pairs favored) and positive values indicate a clustering tendency (Ca–Ca and Mg–Mg pairs favored). The best fit for E_0 was $A_{12} = 49.128$ and $A_{21} = 36.542$ kJ/mol. When only pair, or other even-order (pair=2-, 4-, 6-,…, 2n-body) interactions are used, calculated phase diagrams have mirror symmetry about $x = 0.5$; thus, the E_0 term is the only source of phase diagram asymmetry in this model. The inequality $A_{12} > A_{21}$ reflects the higher energy that is required to substitute larger Ca^{2+} ions into a Mg-rich crystal relative to the smaller energy required to substitute a Mg^{2+} ion into a Ca-rich crystal. This is a well understood phenomenon related to the more rapid increase in the interatomic energy on contraction than on extension. The Js are plotted in Fig. 4 as functions of interatomic separation and listed in Table 1. The interesting feature of Fig. 4 is the large negative value of $J^{(4)}$. This result has been interpreted as reflecting the high stiffness of the structure along the 4th neighbor pair, caused by the presence of rigid CO_3 group

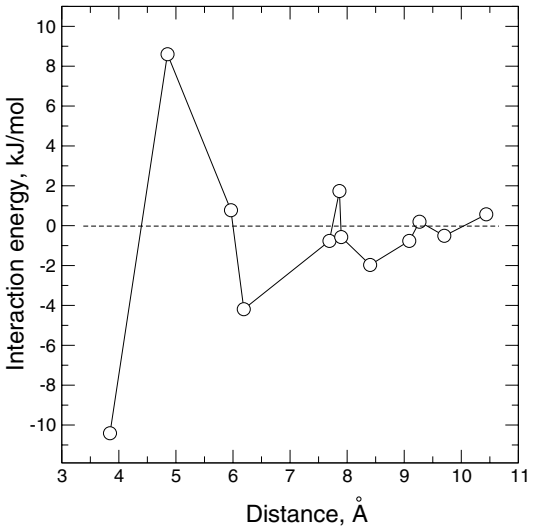

Fig. 4. The cluster expansion of pair-wise effective interactions for the calcite–magnesite system as functions of interatomic separation. The distances have been calculated for a disordered structure with dolomite composition ($a = 19.407$ Å, $c = 15.795$ Å).

Table 1
Pair-wise effective interactions and their type: 1-interlayer, 2-intralayer

n	Distance (Å)	Type	J_n (kJ/mol)
1	3.844	1	−10.200
2	4.852	2	8.563
3	5.964	2	0.931
4	6.190	1	−3.863
5	7.688	2	−0.780
6	7.865	1	1.991
7	7.897	1	−0.982
8	8.403	2	−1.655
9	9.091	2	−0.826
10	9.269	1	−0.111
11	9.703	2	−0.305
12	10.437	1	0.610

between the exchangeable atoms (Vinograd et al., 2006a). A similar phenomenon is observed in pyrope–grossular garnets: the strongest Ca–Mg ordering interactions are $J^{(3)}$ and $J^{(4b)}$, which are distinguished by the presence of SiO_4 and AlO_6 groups, respectively, between the exchangeable cations (Bosenick et al., 2000; Vinograd and Sluiter, 2006). Vinograd and Sluiter (2006) argued that the local stiffness of the structure makes it more energetically unfavorable for long Ca–Ca and short Mg–Mg pairs to accommodate to the average interatomic distance at an intermediate composition. Thus, the dolomite structure maximizes the number of Ca–Mg pairs at the first- and fourth-neighbour distances and minimizes the numbers of nearest neighbor Ca–Ca and Mg–Mg pairs. The Burton and Van de Walle (2003) CE predicts opposite character for $J^{(4)}$, such that it favors Ca–Ca and Mg–Mg 4th neighbor pairs. The essential differences between the CE derived here and the Burton and Van de Walle (2003) CE are that the latter: (1) includes some three-body effective interactions, which determine phase diagram asymmetry; (2) does not include an E_0 term; (3) uses a cross validation score statistical test to chose which clusters to include in the CE, and which VASP structure energies to use for fitting the CE. The cross validation score test is more physically and statistically rigorous than least squares in two ways: (1) the CE is optimized with respect to *formation-energy prediction* rather than minimization of residuals, as in least squares; (2) the number and order (2-, 3-, 4body,…) of effective interactions in the CE is optimized rather than arbitrarily truncated.

The priority in this study is to efficiently calculate activity–composition relations. This requires simulations for both stable and metastable solid solutions, and therefore the suppression of phase separation during simulation runs. To achieve this we adopted a less rigorous CE approach, in which three-body terms are excluded, and the asymmetry of the SSE set is fit with the composition dependent E_0 term, which also absorbs most of the repulsive energy that drives phase separation. Because the E_0 contribution to the free energy is constant at each composition, and the canonical Monte Carlo simulations are performed at constant composition, this approach suppresses phase separation, and allows calculations of the enthalpies and free energies of solid solutions at all compositions. Activities are determined by fitting to the free energies of mixing, and miscibility gaps are calculated from the free energy curvature. Our choice of effective pair interactions includes the first 12 near neighbors (3.8–10.4 Å) which truncates below 1/2 the $4\times4\times1$ supercell dimension along any pair-vector. Because the best CE is not necessarily the one that minimizes residuals, the correction algorithm of Vinograd et al. (2006b) was used to improve the predictive quality of the CE (see below). This procedure is less physically and statistically rigorous than the cross validation score approach (Burton and Van de Walle, 2003), but predicted phase boundaries are in much better agreement with experiment, and activity–composition relations are easily obtained.

5. Ground state analysis

Fig. 3 shows that Eq. (1) yields a good fit to the 700 randomly generated configurations. However, this does not ensure that the CE correctly predicts ground states. Low-energy structures in the $4\times4\times1$ supercell were predicted with Monte Carlo annealing simulations, with the feedback algorithm of Vinograd et al. (2006b): (1) the temperature is set at a high value, then slowly decreased until exchangeable atoms freeze into the state of lowest energy; (2) the GULP–SSE for this structure is calculated, and often this energy differs significantly from the CE-calculated value; (3) the CE is updated with the new structure included and steps (1) and (2) are repeated. The quality of the CE improves automatically. When the energy difference between CE- and GULP-calculated energies is large, the correlation coefficient is significantly reduced and the Js and A_{ij} change to improve the fit. The CE-predicted minima, (including ground states at $x=0$, 1/2, and 1.0) are plotted together with the energies of randomly selected structures in Fig. 2. Consistent with Burton and Van de Walle (2003), calcite, dolomite, calcite + dolomite and dolomite + magnesite are the only stable ground state assemblages. The final CE pair interactions are listed in Table 1. Final values for the E_0 parameters are $A_{12}=46.447$ kJ/mol and $A_{21}=34.151$ kJ/mol; similar to those calculated from the set of randomly selected structures, $A_{12}=49.128$ kJ/mol and $A_{21}=36.542$ kJ/mol.

6. Monte Carlo simulations

Rapid convergence of the CE as a function of interatomic separation (Fig. 4) suggests that Eq. (1) is applicable for calculations of excess energies in a much larger supercell. Sufficient supercell size for thermodynamically meaningful results can be estimated by performing Monte Carlo simulations in supercells of increasing size. The thermodynamic limit is achieved when the predicted properties such as the temperatures of order/disorder transitions converge as functions of supercell size. In Fig. 5 we compare the results

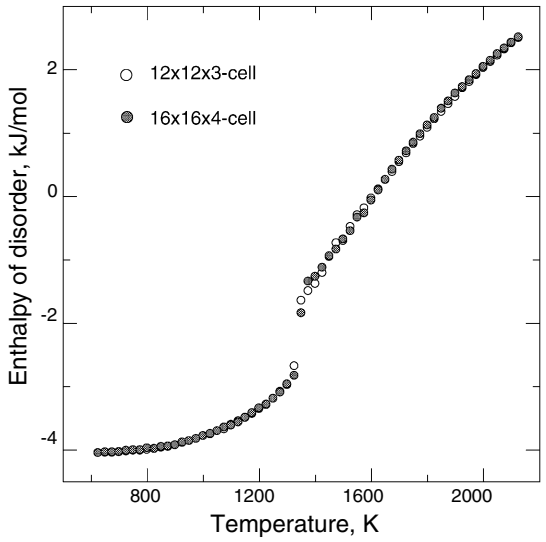

Fig. 5. Enthalpy of disorder at the dolomite composition calculated with the Monte Carlo method. White and shaded symbols correspond to the results obtained with supercells of different size.

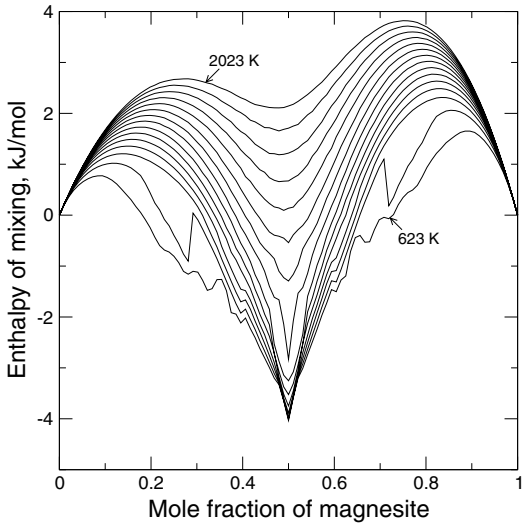

Fig. 6. Enthalpy of mixing isotherms calculated with the Monte Carlo method.

for $12\times12\times3$ and $16\times16\times4$ supercells, which contain 2592 and 6144 exchangeable atoms, respectively. In the both cases the order/disorder transition for dolomite was located between 1323 and 1348 K, which demonstrates that the $12\times12\times3$ supercell is sufficiently large.

At each step of the Monte Carlo run a new configuration is created by swapping randomly chosen pairs of cations. The acceptance probability, ξ, for a candidate configuration depends on temperature, and the energy difference, ΔE, between the two configurations:

$$\xi = 1,\ \Delta E < 0$$
$$\xi = \exp(-\Delta E/(kT)),\ \Delta E > 0 \quad (3)$$

This acceptance rule converges the set of configurations to the Boltzmann distribution (Metropolis et al., 1953). Canonical Monte Carlo simulations were performed on a grid of 48 compositions between calcite and dolomite and 15 temperatures between 623 and 2023 K. Six billion Monte Carlo steps were used to achieve equilibrium and another six billion steps were used to calculate averages. (The five lowest-energy isotherms were simulated with 40 billion MC steps). These simulations were performed with a constant $E_0 = 0$ term; a procedure that necessarily yields the enthalpy of mixing isotherms with mirror symmetry about $x = 0.5$. Composition-dependent E_0 values were subsequently added to the calculated isotherms to get the total asymmetric enthalpy of mixing (Fig. 6).

7. Thermodynamic integration

Myers et al. (1998) and Dove (2001) demonstrated that the configurational free energy can be calculated from Monte Carlo averaged excess energies via λ-integration:

$$F = F_0 + \int_0^{\lambda} E_{\lambda} d\lambda, \quad (4)$$

where F_0 is the free energy of mixing of the solid solution with zero ordering energy, which can be calculated theoretically:

$$F_0 = RT(x_{\mathrm{Mg}} \ln(x_{\mathrm{Mg}}) + x_{\mathrm{Ca}} \ln(x_{\mathrm{Ca}})), \quad (5)$$

where E_λ is the average energy of the system in a state with a non-equilibrium intermediate degree of cation disorder, λ; $0 < \lambda < 1$. λ should not be mixed with the equilibrium order parameter, $Q(T)$, that is a function of temperature. The state $\lambda = 1$ corresponds to an equilibrated system at a given temperature, while the states with $\lambda < 1$ correspond to an artificial disorder that is introduced on top of the equilibrium disorder at the same temperature. This artificial disorder is simulated by scaling the Js according to the equation $J_n^{\lambda} = \lambda J_n$. In our simulations, λ was gradually increased from 0 to 1 with a step size of 0.04. The integral describes the change in free energy of a system at a fixed temperature from the state with zero ordering energy ($\lambda = 0$) to its equilibrium state determined with the nominal values of the Js ($\lambda = 1$). Configurational entropy isotherms were calculated with;

$$S = (F - E)/T \quad (6)$$

and are plotted in Fig. 7. The remarkable features of this plot are the minima at 0.22, 0.28, 0.32, 0.39, 0.5 and the corresponding minima at Mg-rich compositions. The sharp minimum at $x = 0.5$ is caused by dolomite-type ordering, and the minima at $x = 0.22$, 0.28, and0.32 correspond to dolomite-related structures that have different stacking sequences for Ca- and Mg-rich layers. The Monte Carlo simulated low-temperature cation distribution at $x = 0.28$ and $x = 0.32$ (Fig. 8a and b) are consistent with ϵ-dolomite and δ-dolomite (Wenk et al., 1991), respectively, which are layer structures with layer-sequences Mg–Ca–Ca–Ca–$\cdots$ and

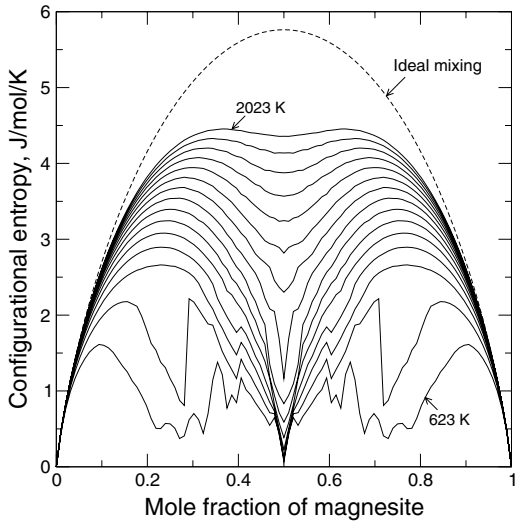

Fig. 7. Configurational entropy isotherms that were calculated by thermodynamic integration.

Mg–Ca–Ca–… perpendicular to c_{hex}. The Mg–Ca–Ca–⋯ sequence is also observed locally at $x = 0.28$, because the supercell with 18 layers in the z direction is incommensurate with the four-layer sequence. This also explains why the energy minimum of ϵ-dolomite is shifted from 0.25 to 0.28. Due to the similar incommensurate relationship, the minimum at $x = 0.22$ corresponds to a structure based on five-layer sequence with the ideal $x = 0.2$ composition. Metastable formation of ϵ-dolomite is consistent with the first principles calculations of Burton and Van de Walle (2003), which suggested that ϵ-dolomite has the lowest formation-energy at $x = 1/4$ and $x = 3/4$. The minimum at $x = 0.39$ corresponds to a structure formed by nearly regularly alternating ordered and antiordered dolomite-type domains (Fig. 8c). The anti-phase boundaries are formed predominanly by Ca atoms which are in excess to the 50:50 ratio. The modulation vector is parallel to the b_{hex} axis. At a slightly more Mg-rich composition, $x = 0.4$, the modulation disappears and the anti-phase boundaries become curved (Fig. 8d).

8. The phase diagram

Free energies of mixing are plotted in Fig. 9. They were converted to a phase diagram by comparing the free energy at each composition x_i along an isotherm to the free energy of a mechanical mixture $x_j + x_k$. If there is a pair of compositions $x_j + x_k$, that has lower free energy, the solution with composition x_i is unstable or metastable (white in Fig. 10) The two miscibility gaps separated by the dolomite field are easily outlined. The calculated diagram is compared to experimental data from Goldsmith (1983), and agreement is nearly quantitative. The difference is that in the calculated diagram the miscibility gap on the Ca-rich side is slightly shifted to more Ca-rich compositions.

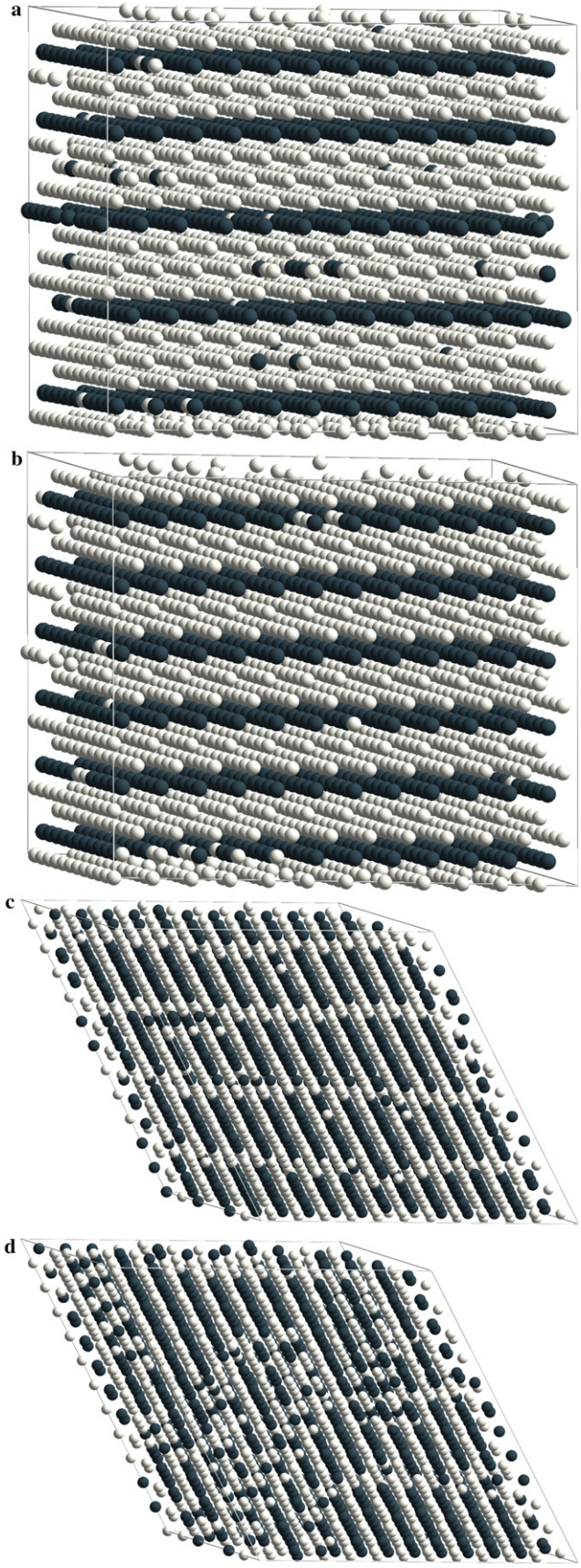

Fig. 8. Monte Carlo simulated cation distributions (Ca-white, Mg-black) at $x = 0.28$ (a), $x = 0.32$ (b), $x = 0.39$ (c), and $x = 0.40$ (d). $T = 623$ K.

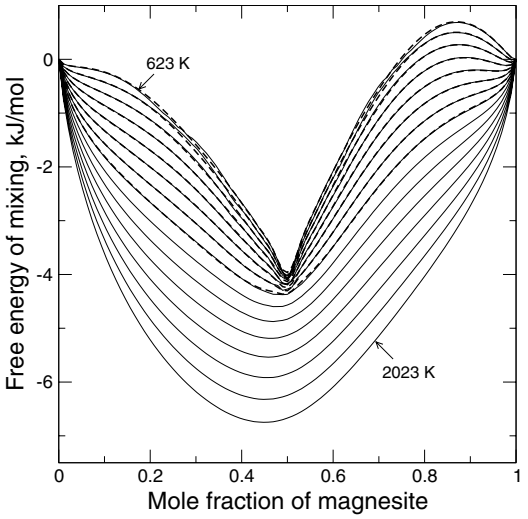

Fig. 9. Free energy of mixing isotherms calculated by thermodynamic integration (solid lines) and fit to this energies using Eq. (7) (dashed lines). The fit applies only to the temperature range 623–1323 K.

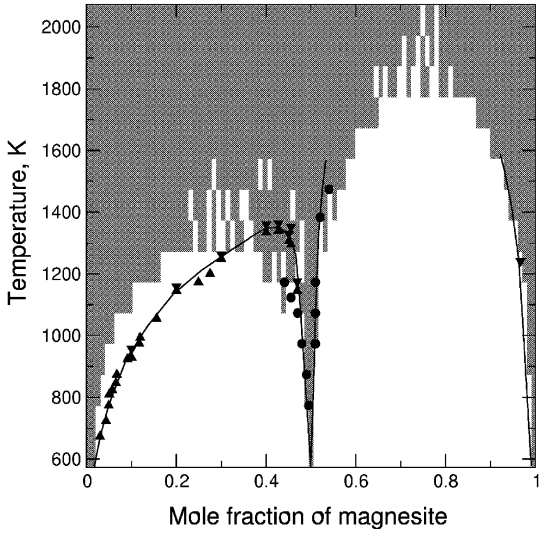

Fig. 10. The calcite–magnesite phase diagram. Gray and white areas indicate stable and unstable (or metastable) states, respectively; predicted by Monte Carlo simulations. Symbols and solid lines are experimental data from Goldsmith (1983). Regions of alternating gray and white bands above the solidus lines are interpreted as being caused by statistical noise.

9. Activity–composition relations

Redlich–Kister polynomials (Redlich and Kister, 1948) are convenient for describing excess free energies of mixing, but these equations fail in systems with strong ordering at intermediate compositions. The rapid decrease in free energy from dolomite-ordering at $x = 0.5$ can be parameterized with negatively shaped Gaussians. The combination of Redlich–Kister polynomials and Gaussians is very effective for fitting free energies of mixing in systems with intense ordering at intermediate compositions (e.g. Vinograd, 2002; Vinograd and Sluiter, 2006). The total excess free energy of mixing can be described with the equation;

$$G_{\text{excess}} = x_1 x_2 \sum_{i=1}^{n} A_i (x_1 - x_2)^{(i-1)} + x_1 x_2 \sum_{j=1}^{m} B_j \times \exp(C_j (x_1 - x_j)^2), \quad (7)$$

where A_i, B_j, and C_j are further expanded as functions of temperature $A_i = A_i^h - TA_i^s$, $B_j = B_j^h - TB_j^s$, $C_j = C_j^h - TC_j^s$; x_1, and x_2 are the mole fractions of end-members and x_j is the mole fraction, of ordered compound j. Fig. 9 illustrates the accuracy of Eq. (7)-fit to Monte Carlo simulated free energies of mixing. The A_i, B_j, and C_j coefficients are listed in Tables 2 and 3. The fit has been performed only in the temperature range of 623–1323 K. Fig. 11 is a plot of activity–composition relations, which were derived from fitted free energies of mixing using the Equations

$$RT \ln \gamma_i = G_{\text{excess}} + (1 - x_i) \frac{\mathrm{d}(G_{\text{excess}})}{\mathrm{d}x_i} \quad (8)$$

and

$$a_i = x_i \gamma_i, \quad (9)$$

where γ_i is the activity coefficient.

10. Discussion and conclusions

Good agreement between predicted and experimentally determined phase relations indicates that the simulations reproduce the main thermodynamic effects of mixing and cation order/disorder in the rhombohedral carbonates. The main difference between experiment and calculation is that the Ca-rich calcite + dolomite field is slightly shifted to more Ca-rich compositions. This might be the result of performing the simulations in the static limit. Burton and van de Walle (2006) demonstrated that including excess vibrational entropy in a first principles phase diagram calculation for the system NaCl–KCl leads to a dramatic improvement in the calculated consolute temperature. However, the Burton and Van de Walle (2003) calculations, which ignored excess vibrational entropy, yielded a critical temperature for cation order-disorder that is about 1.2 times the experimental value, which suggests a modest excess vibrational entropy contribution in this system. Vinograd and Sluiter (2006) have shown that excess vibrational entropy plays a significant role in the subsolidus phase relations of pyrope–grossular, $Mg_3Al_2Si_3O_{12}$–$Ca_3Al_2Si_3O_{12}$, garnets. It has been argued that the positive

Table 2
Coefficients of the Redlich–Kister polynomial (A_i^h in kJ/mol, A_i^s in J/K/mol)

i	A_i^h	A_i^s
1	11.8948	−3.2801
2	6.0778	−0.0866
3	5.6420	−8.5177
4	0.5705	0.5624
5	10.5240	12.4392
6	−0.6759	−0.6519

Table 3
Coefficients of the gaussians (B_j^h and C_j^h in kJ/mol, B_j^s and C_j^s in J/K/mol)

j	x	B_j^h	B_j^s	C_j^h	C_j^s
1	0.5	−16.7374	−10.6106	10.1136	38.8
2	0.5	−5.9028	−4.3690	8.5369	205.1
3	0.5	−3.7182	−2.5465	−447.3994	1276.8

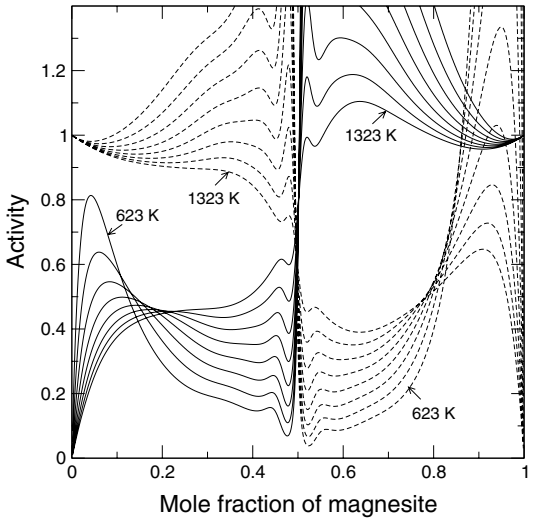

Fig. 11. Fitted activities of calcite and magnesite (solid and dashed lines, respectively) in the interval 623–1323 K. The standard state corresponds to pure calcite or magnesite at the temperature of interest.

excess entropy in the pyrope–grossular system appears as a consequence of the size-mismatch between end-members. Their results also suggested that the maximum of the excess effect is shifted in the direction of the end-member with the largest volume. If the same trend holds for carbonates, the excess entropy would make Ca-rich compositions more stable, and this would improve agreement between calculations and experiment. This assumption should be tested in future simulation studies.

The predicted excess enthalpy for ordered dolomite, −4.0 kJ/mol, is in good agreement with the experimental value, -5.74 ± 0.25 kJ/mol (Navrotsky and Capobianco, 1987) and with the ab initio VASP result, −3.66 kJ/mol, (Burton and Van de Walle, 2003). The predicted equilibrium excess enthalpy of dolomite, −0.5 kJ/mol at 1523 K (Fig. 6), is in reasonable agreement with the value of 1.23 ± 0.32 kJ/mol measured by Navrotsky and Capobianco (1987) for a sample of Eugui dolomite that was heat-treated at 1523 K. The value of 16.5 ± 2.5 kJ/mol measured by Navrotsky et al. (1999) for a synthetic disordered dolomite cannot be explained by the present model. According to our simulations (Fig. 2), a random Ca/Mg configuration contributes only 6–8 kJ/mol to the excess enthalpy of dolomite. The present model also contradicts calorimetric measurements of Chai et al. (1995), which suggested that the enthalpies of formation of diagenetic Ca-rich dolomites are significantly higher than those of isochemical calcite + magnesite mechanical mixtures. Note that our model only includes the effects of the cation order-disorder, and ignores orientational order-disorder of the CO_3 groups. The CO_3-group orientational order-disorder ($R\bar{3}c$/ $R\bar{3}m$) transition in calcite occurs at about 1260 K (Dove and Powell, 1989; Dove et al., 2005). It is possible that some CO_3-group disordering could be quenched during the heat treatments of natural dolomite samples. This effect might explain the difference of 1.72 kJ/mol between the excess energy of the heat-treated dolomite measured by Navrotsky and Capobianco (1987) and our value of −0.5 kJ/mol at 1523 K. The very large value of the excess energy of 16.5 ± 2.5 kJ/mol measured by Navrotsky et al. (1999) for a synthetic dolomite might be caused by orientational disorder. The low temperature of the synthesis (70 °C) might not be sufficient for CO_3 groups to reorder themselves into to the lowest energy configuration. The same argument might apply to the high excess enthalpies of diagenetic Ca-rich dolomites measured by Chai et al. (1995). Density functional calculations of Burton and Van de Walle (2003) have shown the very high energy of formation for huntite-structure $Ca_3Mg(CO_3)_4$ (a structure, in which CO_3-group orientation differs from that of calcite and dolomite). This structure was derived from the naturally occurring $Mg_3Ca(CO_3)_4$ huntite (Dollase and Reeder, 1986) by substituting Ca for Mg and Mg for Ca. The very high formation energy of this structure (44.73 kJ/mol (VASP), 28.72 kJ/mol (GULP)) suggests that even a small concentration of huntite-like domains could significantly increase enthalpies of formation in Ca-rich dolomites. Transmission electron microscopy studies of Ca-rich dolomites in pre-Holocene rocks often reveal modulation with a lamellar spacing of 100–200 Å (Wenk et al., 1983). Crystal structure refinements of two such samples within the $R\bar{3}$ space group of dolomite have shown poor fits and indicated that one of the components of the modulated structure should have mixed occupancy in cation layers (Reeder, 2000). Huntite, $Ca_3Mg(CO_3)_4$, having a mixed (ordered) arrangement of Ca and Mg in dolomite-like cation layers satisfies this criterion. An increase in the fraction of huntite-like domains within the modulated structure could explain the correlation of the excess enthalpies of Ca-rich dolomites with mole fraction of calcite (Chai et al., 1995). This hypothesis should be tested in future simulation studies, and by electron microscopy studies of natural samples. However, the success of the present model in reproducing the phase diagram without accounting for phases with CO_3-group orientational disorder suggests that the miss-orientation of the CO_3-groups plays a minor role in determining equilibrium subsolidus phase relations. The very high formation energy of these structural defects is consistent with the observation of Reeder and Nakajima (1982) that thermal disorder of dolomite produces twin domains boundaries (TDB) rather than anti-phase boundaries (APB). The difference is that an APB implies misaligned CO_3-groups as well as misaligned cation layers, whereas the TDB only has a cation mismatch, without CO_3-group orientational mismatch.

We show that a well-parameterised set of empirical interatomic potentials is sufficient to predict realistic activity–composition relations for the calcite–magnesite system. These simulation tools permit investigation of the system at relatively low temperatures and in highly ordered states, which are not easily accessible by experiment.

Acknowledgments

The present investigation was supported by Deutsche Forschungsgemeinschaft (Project Wi-1232/14-2). J.D.G thank the Government of Western Australia for funding under the Premiers's Research Fellowship program. The calculations were performed at the Center for Scientific Computing at the University of Frankfurt.

Associate editor: Eric H. Oelkers

References

Austen, K., Wright, K., Slater, B., Gale, J.D., 2005. The interaction of dolomite surfaces with metal impurities: a computer simulation study. *Phys. Chem. Chem. Phys.* **7**, 4150–4156.

Becker, U., Fernandez-Gonzalez, A., Prieto, M., Harrison, R., Putnis, A., 2000. Direct calculation of thermodynamic properties of the barite/celectite solid solution from molecular principles. *Phys. Chem. Miner.* **27**, 291–300.

Bosenick, A., Dove, M.T., Geiger, C.A., 2000. Simulation studies on the pyrope–grossular solid solution. *Phys. Chem. Miner.* **27**, 398–418.

Burton, B.P., 1987. Theoretical analysis of cation ordering in binary rhombohedral carbonate systems. *American Mineral.* **72**, 329–336.

Burton, B.P., Kikuchi, R., 1984. Thermodynamic analysis of the system $CaCO_3$–$MgCO_3$ in the tetrahedron approximation of the cluster variation method. *American Mineral.* **69**, 165–175.

Burton, B.P., Van de Walle, A., 2003. First principles based calculations of the $CaCO_3$–$MgCO_3$ subsolidus phase diagrams. *Phys. Chem. Miner.* **30**, 88–97.

Burton, B.P., van de Walle, A., 2006. First principles phase diagram calculations: the role of excess vibrational entropy. *Chem. Geol.* **225**, 222–229.

Chai, L., Navrotsky, A., 1996. Synthesis, characterization, and energetics of solid solution along the $CaMg(CO_3)_2$–$CaFe(CO_3)_2$ join and implication for the stability of ordered $CaFe(CO_3)_2$. *American Mineral.* **81**, 1141–1147.

Chai, L., Navrotsky, A., Reeder, R.J., 1995. Energetics of calcium-rich dolomite. *Geochim. Cosmochim. Acta* **59**, 939–944.

Connolly, J.W.D., Williams, A.R., 1983. Density-functional theory applied to phase transformations in transition-metall alloys. *Phys. Rev.* **B27**, 5169–5172.

Davidson, P.M., 1994. Ternary iron, magnesium, calcium carbonates: a thermodynamic model for dolomite as an ordered derivative of calcite-structure solutions. *American Mineral.* **79**, 332–339.

Dollase, W.A., Reeder, R.J., 1986. Crystal structure refinement of huntite, $Ca_3Mg(CO_3)_4$, with X-ray power data. *American Mineral.* **71**, 163–166.

Dove, M.T., 1999. Order/disorder phenomena in minerals: ordering phase transitions and solid solutions. In: Wright, K., Catlow, R. (Eds.), *Microscopic properties and processes in minerals*, *NATO ASI Ser. C*, 543. Kluwer, Dordrecht, pp. 451–475.

Dove, M.T., 2001. Computer simulations of solid solutions. In: Geiger, Ch. (Ed.), *Solid Solutions in Silicate and Oxide Systems of Geological Importance*, *EMU Notes in Mineralogy*, 3. Eötvös University Press, Budapest, pp. 245–249.

Dove, M.T., Powell, B.M., 1989. Neutron powder diffraction study of the tricritical orientational order-disorder phase transition in calcite at 1260 K. *Phys. Chem. Miner.* **16**, 503–507.

Dove, M.T., Swainson, I.P., Powell, B.M., Tennant, D.C., 2005. Neutron powder diffraction study of the orientational order-disorder phase transition in calcite, $CaCO_3$. *Phys. Chem. Miner.* **32**, 493–503.

Ferreira, L.G., Mbaye, A.A., Zunger, A., 1988. Chemical and elastic effects on isostructural phase diagrams: The e-G approach. *Phys. Rev. B* **37**, 10547–10570.

Goldsmith, J.R., 1983. Phase relations of rhombohedral carbonates. In: Reeder, R.J. (Ed.), *Reviews in Mineralogy*, 11, pp. 49–76.

Gale, J.D., 1997. GULP–a computer program for the symmetry adapted simulation of solids. *J. Chem. Soc.: Faraday Trans.* **93**, 629–637.

Gale, J.D., Rohl, A.L., 2003. The general utility lattice program (GULP). *Mol. Simulations* **29**, 291–341.

Goldsmith, J.R., Heard, H.C., 1961. Subsolidus phase relations in the system $CaCO_3$–$MgCO_3$. *J. Geol.* **80**, 611–626.

Kresse, G, Hafner, J, 1993. Ab initio molecular dynamics for liquid metals. *Phys. Rev.* **B47**, 558–561.

Kresse, G. (1994) Thesis, Technische Universität Wien 1993. *Phys. Rev.,* **B49**, 14251

Kresse, G., & Furthmüller, J. (1996). Efficiency of ab-initio total energy calculations for metals and semiconductors using a plane-wave basis set. *Comput. Mat. Sci.,* **6**, 15–50; Efficient iterative schemes for ab initio total-energy calculations using a plane-wave basis set. *Phys. Rev.,***B54**, 11169. cf. <http://tph.tuwien.ac.at/vasp/guide/vasp.html./>.

Metropolis, N.I., Rosenbluth, A.W., Rosenbluth, M.N., Teller, A.N., Teller, E., 1953. Equation of state calculations by fast computing machines. *J. Chem. Phys.* **21**, 1087–1092.

Myers, E.R., Heine, V., Dove, M.T., 1998. Some consequences of Al/Al avoidance in the ordering of Al/Si tetrahedral framework structures. *Phys. Chem. Miner.* **25**, 457–464.

Navrotsky, A., 1987. Models of crystalline solutions. In: Reeder, R.J. (Ed.), *Rewiews in Mineralogy*, Vol. 17. Mineralogical Society of America, Washington DC.

Navrotsky, A., Capobianco, C., 1987. Enthalpies of formation of dolomite and of magnesian calcites. *American Mineral.* **72**, 782–787.

Navrotsky, A., Dooley, D., Reeder, R., Brady, P., 1999. Calorimetric studies of the energetics of order-disorder in the System Mg_xFe_{1-x}-$Ca(CO_3)_2$. *American Mineral.* **84**, 1622–1626.

Purton, J.A., Allan, N.L., Lavrentiev, M.Yu., Todorov, I.T., Freeman, C.L., 2006. Computer simulation of mineral solid solutions. *Chem. Geol.* **225**, 176–188.

Reeder, R.J., 2000. Constraints on cation order in calcium-rich sedimentary dolomite. *Aquat. Geochem.* **6**, 213–226.

Reeder, R.J., Nakajima, Y., 1982. The nature of ordering and ordering defects in dolomite. *Phys. Chem. Miner.* **8**, 29–35.

Redlich, O., Kister, A.T., 1948. Thermodynamics of non-electrolyte solutions, *x-y-t* relations in a binary system. *Ind. Eng. Chem.* **40**, 341–345.

Rohl, A.L., Wright, K., Gale, J.D., 2003. Evidence from surface phonons for the (2×1) reconstruction of the (10–14) surface of calcite from computer simulation. *American Mineral.* **88**, 921.

Sanchez, J.M., Ducastelle, F., Gratias, D., 1984. Generalized cluster description of multicomponent systems. *Physica* **128A**, 334–350.

Vinograd, V.L., 2001. Configurational entropy of binary silicate solid solutions. In: Geiger, Ch. (Ed.), *Solid Solutions in Silicate and Oxide Systems of Geological Importance*, *EMU Notes in Mineralogy*, 3. Eötvös University Press, Budapest, pp. 303–346.

Vinograd, V.L., 2002. Thermodynamics of mixing and ordering in the diopside-jadeite system: II. A polynomial fit to the CVM results. *Mineral. Mag.* **66**, 537–545.

Vinograd, V.L., Sluiter, M.H.F., 2006. Thermodynamics of mixing in pyrope–grossular, $Mg_3Al_2Si_3O_{12}$–$Ca_3Al_2Si_3O_{12}$, solid solution from lattice dynamics calculations and Monte Carlo simulations. *American Mineral.* **91**, 1815–1830.

Vinograd, V.L., Winkler, B., Putnis, A., Gale, J.D., Sluiter, M.H.F., 2006a. Static lattice energy calculations of mixing and ordering

enthalpy in binary carbonate solid solutions. *Chem. Geol.* **225**, 304–313.

Vinograd, V.L., Winkler, B., Putnis, A., Kroll, H., Milman, V., Gale, J.D., et al., 2006b. Thermodynamics of pyrope–majorite, $Mg_3Al_2Si_3O_{12}$–$Mg_4Si_4O_{12}$, solid solution from atomistic model calculations. *Mol. Simulations* **32**, 85–99.

Wenk, H.-R., Barber, D.J., Reeder, R.J, 1983. Microstructures in carbonates. In: Reeder, R.J. (Ed.), *Reviews in Mineralogy*, Vol. 11, pp. 301–367.

Wenk, H-R., Meisheng, Hu., Lindsley, T., Morris Jr., J.W., 1991. Superstructures in ankerite and calcite. *Phys. Chem. Miner.* **17**, 527–539.